LANGMUIR

pubs.acs.org/Langmuir Article

Criteria of Distribution Transitions in Dispersed Multiphase Systems Based on an Extended Lattice Model

Yiran Li, Yunfan Huang, Xukang Lu, and Moran Wang*

Cite This: *Langmuir* 2023, 39, 17021−17030 Read Online

ACCESS | Metrics & More | Article Recommendations | Supporting Information

ABSTRACT: Dispersed multiphase systems are ubiquitous in biological systems, energy industries, and medical science. The distribution transition of the dispersed phase is critical to the properties and functions of the multiphase systems, among which the agglomeration, adsorption, and extraction processes are of most significance due to their impact on the colloidal stability, interface modification, and particle synthesis. To reveal fundamental correlations between the macroscopic particle distributions and the microscopic interactions, general thermodynamic models of the dispersed multiphase systems are needed. Here, based on Meyer's model, which is restricted to binary isotropic mixtures, we propose a novel extended lattice model that can be applied to multicomponent anisotropic mixtures with interfaces considered. For agglomeration, adsorption, and extraction processes, the approximate free energy differences between the initial distribution and the final distribution are obtained. Based on the minimum free energy principle, the above free energy differences are used to derive three criteria for the prediction of the preferable distribution of the system with given interparticle interaction potentials. While the quasi-uniform number density assumption is still required for all the previous lattice models, the long-range interactions neglected by previous lattice models are incorporated. The validity of our model and criteria is verified by many-body dissipative particle dynamics (mDPD) simulations. By tuning the interaction coefficients between mDPD particles, the simulated distribution transitions for all the agglomeration, adsorption, and extraction cases perfectly match the predictions from the three criteria. The good agreement between the theoretical predictions and the mDPD simulation results shows the great potential of our model for applications in various dispersed multiphase systems.

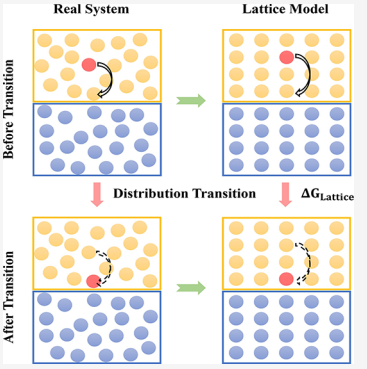

INTRODUCTION

Dispersed multiphase systems are mixtures consisting of immiscible phases with at least one component existing as a discrete phase.[1,2] These mixtures are ubiquitous in biological systems, energy industries, and medical science.[3−5] The distribution of the dispersed components in mixtures, such as blood cells and platelets in human blood, nanoparticles in nanofluids,[6] and nanomicelles in nanoemulsions is influential in the human's cardiovascular system,[7] oil recovery efficiency,[8,9] and dermatological treatment.[10] Among various distributions of dispersed particles, agglomeration, adsorption, and extraction at interfaces of immiscible fluids have garnered increased interest among researchers.[11−15] The stability of nanofluids is the crucial premise for its various industrial applications,[16] which depends on the agglomeration propensity of nanoparticles[17,18] and could be affected by pH values of base fluids,[19] particle concentration,[20] and particle size.[21] The nanoparticle adsorption at liquid−liquid interfaces and solid surfaces is a dominant mechanism to enhance the oil recovery rate[8] and can be influenced by the shape, surface property, and charge of nanoparticles.[22−25] Besides, particle extraction through the liquid−liquid interface, which is critical in nanotechnologies like quantum dots and nanoparticles, has also been intensively investigated.[26−28] Although plenty of efforts have been devoted to the study of the three typical distributions in multiphase systems, most of the existing theories and models are limited to specific systems,[23,25,29−32] resulting in the limitation of lacking universal applicability. A general theory of dispersed multiphase system including analysis for all three distributions is thus needed.

A dispersed multiphase system is essentially a thermodynamic system consisting of interacting particles of different types, based on which an adsorption theory that applies to multiple binary mixtures including water-sulfuric acid, hydrogen-palladium, argon-graphite, etc., was proposed by Hill in 1949.[33] Despite its ability to quantitatively describe the thermodynamic properties of the system from experimental data, this theory does not provide enough insight into the relationship between microscopic interactions and macroscopic distributions of particles, which is critical for the design of novel nanomaterials.[8,24,26] Theoretically, the macroscopic equilibrium distribution of the dispersed particles can be

Received: June 10, 2023
Revised: November 11, 2023
Accepted: November 12, 2023
Published: November 22, 2023

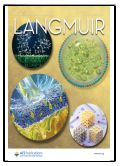

obtained by searching the minimum free energy point in the phase space of the system when all of the interparticle interactions are known. Nevertheless, due to the unstructured nature of the mixture, it is impracticable to obtain the analytic expression of the system's free energy.

To uncover the underlying dominant rules in the dispersed multiphase system through the facade of randomness, approximate models are required. Lattice models were proposed and extensively employed by previous researchers to analytically investigate complex systems, such as the Ising model predicting the phase transition of physical systems and lattice gas cellular automata (LGCA) describing the emergent behavior of fluid transport.[34−36] An idealized lattice model for binary mixtures was first constructed by Meyer, assuming a lattice structure in the liquid with lattice constants independent of the composition,[37] from which the entropy of mixing for two different ideal liquids with the same number densities was correctly derived.[38] Further modified versions of Meyer's model, including regular solution theory and Flory−Huggins theory, were proposed and succeeded in explaining phase separation phenomena in nonideal solutions and polymer mixtures.[37−39] However, all of the above lattice models are confined to binary systems and thus are not applicable to investigate phenomena in ternary mixtures, including the interfacial adsorption and phase transfer process of particles. Although the distribution transitions in both binary and ternary systems are discussed by Israelachvili,[40] there is no strict theoretical basis for the derivation of the analytically expressed energy differences between different distributions.

In the present work, under the quasi-uniform local number density assumption made by both the Ising model and the regular solution theory,[38] we extend the lattice model to describe multicomponent systems in thermodynamic equilibrium and propose a method to approximate the free energy of the real system, whereby semiquantitative criteria of distribution transitions of the three phenomena discussed above are expressed with interparticle potential parameters. To verify the theory, constructing simulation systems corresponding to the three distribution transitions is the most direct and effective way. Many-body dissipative particle dynamics (mDPD), as a mesoscale simulation method widely used in colloidal and interfacial science,[41−45] has several main advantages when applied to study complex fluids and colloidal solutions, such as its interparticle soft potential which significantly improves its computational efficiency, and the truly meshfree particle-based feature appropriate for simulating moving interfaces.[46] This method is employed to model binary and ternary mixtures for verification of our model and distribution transition criteria. The good agreement between the theoretical predictions and the mDPD simulation results shows the great potential of our model for applications in dispersed multiphase systems such as innovative nanoparticle synthesis, colloid system characterization, and parameter control in particle-based simulations.

MATERIALS AND METHODS

Extended Lattice Model: Approximate of the Helmholtz Free Energy Difference. We first propose a novel lattice model that can be applied to multiphase dispersed systems with quasi-uniform local number densities. With the assumed lattice structure, the approximate Helmholtz free energy of the system is expressed as a function of the particle distribution and interparticle interactions and used to calculate the free energy difference between systems with different distributions.

For a particle system composed of M types of particles and with almost uniform local number densities, the widely used lattice model can be employed, which assumes that each particle occupies one lattice site without overlapping with a hypothetical simple cubic lattice. While the lattice constant a could be arbitrarily chosen in Meyer's model, here it is uniquely determined by the average number density n of the particle system, satisfying

$$\frac{1}{a^3} = n \tag{1}$$

which is analogous to the treatment of the cell model in colloid science.[47,48] Since the lattice structure of the system is assumed, the possible spacings between particles comprise a discrete set and thus can be ordered. The αth closest spacing between particles is denoted by r_α. And for each particle, the number of neighbors at a distance of r_α from it is denoted by c_α. The particle pairs consisting of a type-i particle and a type-j particle with spacing r_α are called "i-j type αth closest" pairs, and the interaction energy of such pairs is denoted by u_α^{ij}. The particle distribution is characterized by the set of numbers representing the number of each type of pair, $\{N_\alpha^{ij}\}$. To calculate the interaction energy of a certain distribution, our model incorporates the interactions between all the particle pairs in the system, instead of restricting the interparticle interactions to nearest particle pairs as Meyer did. The total interaction energy U^{pot} can then be written as

$$U^{\mathrm{pot}} = \sum_{\alpha=1}^{\infty}\sum_{i=1}^{M}\sum_{j=1}^{i} N_\alpha^{ij} \times u_\alpha^{ij} \tag{2}$$

which is determined by both the number N_α^{ij} and the energy u_α^{ij} of each type of pair. In contrast, the entropy of the system with a certain type of particle distribution depends on the number of microscopic states that belong to this distribution, which is determined only by the set $\{N_\alpha^{ij}\}$, so is the entropy $S \equiv S(\{N_\alpha^{ij}\})$. For two different distributions of systems A and B specified by $\{N_\alpha^{ij}\}$ and $\{N_\alpha^{ij'}\}$, respectively, the differences in the total interaction energy and the entropy between them are

$$\Delta U^{\mathrm{pot}} = U^{\mathrm{pot}} - U^{\mathrm{pot}\prime} = \sum_{\alpha=1}^{\infty}\sum_{i=1}^{M}\sum_{j=1}^{l} (N_\alpha^{ij} - N_\alpha^{ij\prime}) \times u_\alpha^{ij} \tag{3}$$

$$\Delta S = S - S' = S(\{N_\alpha^{ij}\}) - S(\{N_\alpha^{ij\prime}\}) \tag{4}$$

Assuming the internal and kinetic energies of particles are independent of interparticle interactions, as in Meyer's model, the difference of the Helmholtz free energy between distributions A and B at a temperature T is obtained as

$$\begin{aligned}\Delta F &= \Delta U^{\mathrm{total}} - T\Delta S = \Delta U^{\mathrm{pot}} - T\Delta S \\ &= \sum_{\alpha=1}^{\infty}\sum_{i=1}^{M}\sum_{j=1}^{i} (N_\alpha^{ij} - N_\alpha^{ij\prime}) \times u_\alpha^{ij} \\ &\quad - T(S(\{N_\alpha^{ij}\}) - S(\{N_\alpha^{ij\prime}\}))\end{aligned} \tag{5}$$

In the canonical ensemble, the preferable distribution of the system is determined by the sign of ΔF; if $\Delta F < 0$, distribution A is preferred and vice versa. As shown in eq 5, the distribution is determined by the competition between the energy effect

https://doi.org/10.1021/acs.langmuir.3c01579
Langmuir 2023, 39, 17021−17030

and the entropy effect. Although the exact form of the entropy difference ΔS is difficult to obtain, it will be presented in subsequent sections that significant information can be drawn from eq 5 to give rather simple criteria expressed by potential parameters to predict and control the particle distribution. In this contribution, we focus on the energy effect and aim to correlate the complex distribution transition phenomena in multicomponent systems with explicit criteria.

Criteria of Distribution Transition under the Locality Assumption. The interactions between macromolecules, colloidal particles, and surfaces decay very fast when compared to their sizes,[40] which indicates that interactions between nonnearby particles are usually negligible. Motivated by the above fact, the locality assumption, which only considers the interaction between closest particles and neglects the rest of the interactions between particle pairs with spacings larger than r_1 is made for simplicity, as in Meyer's model.

Under the locality assumption, eq 5 is simplified as the following form:

$$\Delta F = \Delta U^{\text{total}} - T\Delta S = \Delta U^{\text{pot}} - T\Delta S = \sum_{i=1}^{M}\sum_{j=1}^{i}(N_1^{ij} - N_1^{ij\prime})\cdot u_1^{ij} - T(S(\{N_1^{ij}\}) - S(\{N_1^{ij\prime}\})) \tag{6}$$

which is then applied to binary systems to derive the criteria for the agglomeration process and also used in ternary systems to investigate the adsorption and extraction processes. Following the procedure in the regular solution theory,[38] the interdependent set $\{N_\alpha^{ij}\}$ is reduced to a new set of independent variables using geometrical constraints from the lattice, and then the Helmholtz free energy differences between two different distributions in binary and ternary systems can be, respectively, expressed as

$$\Delta F = -(u_1^{11} + u_1^{22} - 2u_1^{12})\frac{\Delta N_1^{12}}{2} - T(S(\{N_1^{ij}\}) - S(\{N_1^{ij\prime}\})) \tag{7}$$

$$\Delta F = \sum_{\substack{m,n=1\\ m\neq n}}^{3}\left[-(u_1^{mm} + u_1^{nn} - 2u_1^{mn})\frac{\Delta N_1^{mn}}{2}\right] - T(S(\{N_1^{ij}\}) - S(\{N_1^{ij\prime}\})) \tag{8}$$

where $\Delta N_1^{mn} = N_1^{mn} - N_1^{mn\prime}$. Equations 7 and 8 are then employed to calculate the free energy variations during the three types of distribution transitions and derive the corresponding criteria, which are listed in Table 1. It is noteworthy that for the latter two criteria, an additional assumption of a dilute dispersed system is made, which assumes that no 1−1 type pairs exist and reduces the degree of freedom in the analysis. More detailed derivations can be found in Supporting Information Sections 1.1−3.

Table 1. Definition of the Determinants $\Delta_i^0 = F_i^0 - K_{c,i}^0$ of Distribution Transitions under Locality Assumption

number i	phenomena	energy factor F_i^0	entropy factor $K_{c,i}^0$
1	agglomeration	$u_1^{11} + u_1^{22} - 2u_1^{12}$	$-\frac{T\Delta S}{\Delta N_1^{12}/2}$
2	adsorption	$u_1^{22} + u_1^{13} - u_1^{12} - u_1^{23}$	$-\frac{T\Delta S}{N^{(1)}}$
3	extraction	$u_1^{22} + 2u_1^{13} - u_1^{33} - 2u_1^{12}$	$-\frac{T\Delta S}{3N^{(1)}}$

As shown in Table 1, the scaled free energy variations during the distribution transitions, which are defined as the determinants of the transitions, $\Delta_i^0 = F_i^0 - K_{c,i}^0$, are decomposed into two parts: the energy factors F_i^0 and the entropy factors $K_{c,i}^0$. The energy factors are presented as linear combinations of the interaction energies of different particle pairs, while the entropy factors only depend on the distribution difference and hence are constants for given distribution transitions. The signs of the determinants Δ_i^0 are used to determine the preferable distributions. Hence, according to Table 1, the ways that interparticle interactions affect the three types of distribution transitions are obtained. Note that the derived agglomeration energy factor for a binary mixture is consistent with the interfacial tension or the interfacial energy formulation in the previous studies,[37,38] while the latter two energy factors for adsorption and extraction are strictly derived for the first time. The mathematical forms are quite physically intuitive, consistent with the operational thermodynamic considerations[40] but have a more solid statistical foundation with the flexibility for further extension.

Criteria of Distribution Transition for Long-Range Interactions. When investigating molecular systems, the long-range interactions, such as the Coulomb forces, are not negligible, so the locality assumption no longer holds. Without the locality assumption, the free energy differences between different distributions A and B in binary and ternary systems are then expressed as

$$\Delta F = \sum_{\alpha=1}^{\infty}\left(-(u_\alpha^{11} + u_\alpha^{22} - 2u_\alpha^{12})\frac{\Delta N_\alpha^{12}}{2}\right) - T(S(\{N_\alpha^{ij}\}) - S(\{N_\alpha^{ij\prime}\})) \tag{9}$$

$$\Delta F = \sum_{\alpha=1}^{\infty}\sum_{\substack{m,n=1\\ m>n}}^{3}\left[-(u_\alpha^{mm} + u_\alpha^{nn} - 2u_\alpha^{mn})\frac{\Delta N_\alpha^{mn}}{2}\right] - T(S(\{N_\alpha^{ij}\}) - S(\{N_\alpha^{ij\prime}\})) \tag{10}$$

where the interaction energy terms of particle pairs at different spacings are coupled and determine the distribution together, leading to complex expressions of the energy factors which cannot be easily utilized to predict the distribution analytically. To overcome this problem, a constraint on the form of the interparticle potential $u^{ij}(r)$ is imposed as compensation:

$$u^{ij}(r) = A^{ij}w(r) + v(r) \tag{11}$$

where A^{ij} denotes the strength of the first potential term which varies among different types of particle pairs, while functions $w(r)$ and $v(r)$ are the same for all the particle pairs. The most common potentials encountered in chemistry are in the above form, such as the Coulomb potential and the Lennard-Jones potential. Hence, this constraint will not significantly limit the applicability of the theory. With interparticle interactions in the above form, the free energy differences can be rewritten as

$$\Delta F = -(A^{11} + A^{22} - 2A^{12})\sum_{\alpha=1}^{\infty}(w(r_\alpha)\frac{\Delta N_\alpha^{12}}{2}) - T\Delta S \tag{12}$$

https://doi.org/10.1021/acs.langmuir.3c01579
Langmuir 2023, 39, 17021−17030

Table 2. Definition of the Determinants $\Delta_i = F_i - K_{c,i}$ of Distribution Transitions with the Form of Interparticle Potential Being $u^{ij}(r) = A^{ij}w(r) + v(r)$

number i	phenomena	energy factor F_i	entropy factor $K_{c,i}$
1	agglomeration	$A^{11} + A^{22} - 2A^{12}$	$-\frac{T\Delta S}{\sum_{\alpha=1}^{\infty}\left(w(r_\alpha)\frac{\Delta N_\alpha^{12}}{2}\right)}$
2	adsorption	$A^{22} + A^{13} - A^{12} - A^{23}$	$-\frac{T\Delta S}{\sum_{\alpha=1}^{\infty}(w(r_\alpha)\Delta N_\alpha^{12})}$
3	extraction	$A^{22} + 2A^{13} - A^{33} - 2A^{12}$	$-\frac{T\Delta S}{\sum_{\alpha=1}^{\infty}\left(w(r_\alpha)\frac{\Delta N_\alpha^{12}}{2}\right)}$

$$\Delta F = \sum_{\substack{m,n=1\\ m>n}}^{3}\left[-(A^{mm} + A^{nn} - 2A^{mn})\sum_{\alpha=1}^{\infty} w(r_\alpha)\frac{\Delta N_\alpha^{mn}}{2}\right] - T\Delta S \tag{13}$$

where $\Delta S = S(\{N_\alpha^{ij}\}) - S(\{N_\alpha^{ij'}\})$.

Following a similar statistical treatment in the previous subsection, the results are obtained and are listed in Table 2. For the agglomeration phenomena, the derivation is in the same manner as the case under 1-locality assumption, while the detailed derivations of the latter two can be found in Supporting Information Section 1.4. The energy factors F_i's here share the isomorphic forms with the ones in Table 1, which is the natural corollary by the constrained form of the interparticle potentials. As we will see in the next section, this formulation plays an important role in modeling and predicting the behaviors of mDPD systems.

Short Overview of the mDPD System. The proposed lattice model is further applied to mDPD systems. In this section, a brief introduction to mDPD systems is given.

An mDPD system consists of N interacting particles, whose positions and velocities are denoted by $\boldsymbol{r}_i$ and $\boldsymbol{v}_i$, respectively, evolving under the control of Newtown's law of motion

$$\frac{d\boldsymbol{r}_i}{dt} = \boldsymbol{v}_i, \quad \frac{d\boldsymbol{v}_i}{dt} = \frac{\boldsymbol{F}_i}{m_i} \tag{14}$$

where m_i is the mass of particle i. The total force acting on particle i, F_i, is composed of external force $\boldsymbol{F}_i^{ext}$ and the sum of pairwise forces F_{ij} owing to the interaction between particles i and j, namely

$$\boldsymbol{F}_i = \boldsymbol{F}_i^{ext} + \sum_{i\neq j}\boldsymbol{F}_{ij} \equiv \boldsymbol{F}_i^{ext} + \sum_{i\neq j}(\boldsymbol{F}_{ij}^{C} + \boldsymbol{F}_{ij}^{D} + \boldsymbol{F}_{ij}^{R}) \tag{15}$$

where the superscripts in the pairwise force terms denote the conservative force, dissipative force, and random force, respectively

$$\begin{aligned}\boldsymbol{F}_{ij}^{C} &= A_{ij}w_c(r_{ij})\hat{\boldsymbol{r}}_{ij} + B(\overline{\rho}_i + \overline{\rho}_j)w_d(r_{ij})\hat{\boldsymbol{r}}_{ij}\\ \boldsymbol{F}_{ij}^{D} &= -\gamma w_D(r_{ij})(\boldsymbol{v}_{ij}\times\hat{\boldsymbol{r}}_{ij})\hat{\boldsymbol{r}}_{ij}\\ \boldsymbol{F}_{ij}^{R} &= \sigma w_R(r_{ij})\zeta_{ij}\hat{\boldsymbol{r}}_{ij}\end{aligned} \tag{16}$$

where $\hat{\boldsymbol{r}}_{ij} = \boldsymbol{r}_{ij}/r_{ij}$ and $\boldsymbol{v}_{ij} = \boldsymbol{v}_i - \boldsymbol{v}_j$. The weight functions in the expression of conservative force are determined according to previous mDPD studies,[44,49,50] $w_c(r_{ij}) = (1 - r_{ij}/r_c)H(r_{ij} - r_c)$ and $w_d(r_{ij}) = (1 - r_{ij}/r_d)H(r_{ij} - r_d)$, which vanish when $r > r_c$ and $r > r_d$ ($H(x)$ is the Heaviside function), respectively, while w_D and w_R satisfy $w_D = w_c^2$ and $w_R = w_c$. The interparticle conservative potential parameter $A_{ij} < 0$ governs the magnitude of the attractive part which could differ for different types of particle pairs, while $B > 0$ controlling the amplitude of the repulsive part is necessary a constant for all particle pairs to ensure the mDPD system evolves as a Hamiltonian system.[51] The weighted density $\overline{\rho}_i$ is defined as

$$\overline{\rho}_i = \sum_{j\neq i} w_\rho(r_{ij}) \equiv \sum_{j\neq i}\frac{15}{2\pi r_d^3}\left(1 - \frac{r_{ij}}{r_d}\right)^2 H(r_{ij} - r_d) \tag{17}$$

which vanishes for $r > r_d$. γ and σ are the amplitudes of the dissipative and random forces. ζ_{ij} is a Gaussian random noise with $\langle\zeta_{ij}(t)\rangle = 0$ and $\langle\zeta_{ij}(t)\zeta_{kl}(t')\rangle = (\delta_{ik}\delta_{jl} + \delta_{il}\delta_{jk})\delta(t - t')$. In addition, the fluctuation−dissipation relation $\sigma^2 = 2\gamma k_B T$ is imposed on the random and dissipative coefficients to keep the equilibrium distribution of the mDPD system the same as that of a Hamiltonian system with conservative interactions $\boldsymbol{F}_i^C$ only,[52] indicating the effectiveness of all the standard thermodynamic relations including the entropy effects in mDPD systems, which is the prerequisite for the application of our lattice model.

Extended Lattice Model of mDPD Systems. In most mDPD models constructed in previous studies, the average number density n ranges from 5 to 10. According to eq 1, the corresponding lattice constant a is in the range of 0.45 to 0.6. Given that conventionally the cutoff distance r_c is set to the unit of length in mDPD studies,[52] namely, $r_c = 1 \doteq 2a$, $\{r_\alpha\}$ and $\{c_\alpha\}$ are thus determined as

$$r_1 = \frac{1}{2}r_c, \quad r_2 = \frac{\sqrt{2}}{2}r_c, \quad r_3 = \frac{\sqrt{3}}{2}r_c, \quad c_1 = 6, \quad c_2 = 12, \quad c_3 = 8 \tag{18}$$

where the 3-locality assumption, in which only the interactions between the first three closest pairs are considered, has been adopted.

As mentioned before, the equilibrium distribution of the mDPD system is the same as that of a Hamiltonian system with conservative interactions $\boldsymbol{F}_i^C$ only. Hence, for mDPD particle pairs, the interactional energy could be obtained by summing the attractive and repulsive contribution. For the attractive part, the potential could be directly obtained by integrating the attractive force against displacement

$$u_A^{ij}(r) = \int_r^\infty F_{A_{ij}}{}^C(\zeta)d\zeta = A_{ij}\int_r^\infty w_c(\zeta)d\zeta \tag{19}$$

For the repulsive interaction, the total many-body potential is a sum of density-dependent one-body terms[51]

$$U_R = \frac{1}{2}B\sum_i \overline{\rho}_i^2 \tag{20}$$

Using the expression of the weighted density (eq 17), the total repulsive potential could be written as the sum of "pairwise" potential:

https://doi.org/10.1021/acs.langmuir.3c01579
Langmuir 2023, 39, 17021−17030

$$U_R = \frac{1}{2}B\sum_i \overline{\rho}_i^2 = \frac{1}{2}B\sum_{i\neq j}\frac{1}{2}(\overline{\rho}_i + \overline{\rho}_j)w_\rho = B\sum_{i>j}\frac{1}{2}(\overline{\rho}_i + \overline{\rho}_j)w_\rho = \sum_{i>j}u_R^{ij}(r) \quad (21)$$

Since the number density is uniform and homogeneous $\overline{\rho}_i \equiv \overline{\rho}$ in the lattice model, u_R^{ij} can be further expressed as follows:

$$u_R^{ij}(r) = B\overline{\rho}w_\rho(r) \quad (22)$$

Hence, the conservative interparticle interaction energy is:

$$u^{ij}(r) = u_A^{ij}(r) + u_R^{ij}(r) = A_{ij}\int_r^\infty w_c(\zeta)d\zeta + B\overline{\rho}w_\rho(r) \quad (23)$$

eq 23 shows that the mDPD interaction potential is in the required form (eq 11) where:

$$A^{ij} = A_{ij}$$
$$w(r) = \int_r^\infty w_c(\zeta)d\zeta$$
$$v(r) = B\overline{\rho}w_\rho(r) \quad (24)$$

Hence, all the results are presented in Section II.C is applicable to mDPD systems. In particular, the three mDPD coefficient combinations, which, respectively, control the distribution transitions of agglomeration, adsorption, and extraction processes are acquired:

$$F_1 = A_{11} + A_{22} - 2A_{12}$$
$$F_2 = A_{22} + A_{13} - A_{12} - A_{23}$$
$$F_3 = A_{22} + 2A_{13} - A_{33} - 2A_{12} \quad (25)$$

In addition, the transition points could be further expressed as:

$$K_{c,1} = -\frac{T\Delta S}{\sum_{\alpha=1}^\infty\left(w(r_\alpha)\frac{\Delta N_\alpha^{12}}{2}\right)} = -\frac{T\Delta S}{\frac{3}{8}\frac{\Delta N_1^{12}}{2} + \frac{-1+2\sqrt{2}}{4}\frac{\Delta N_2^{12}}{2} + \frac{-3+4\sqrt{3}}{8}\frac{\Delta N_3^{12}}{2}}$$
$$K_{c,2} = -\frac{T\Delta S}{\sum_{\alpha=1}^\infty(w(r_\alpha)\Delta N_\alpha{}^{12})} = -\frac{T\Delta S}{\frac{3}{8}\Delta N_1{}^{12} + \frac{-1+2\sqrt{2}}{4}\Delta N_2{}^{12} + \frac{-3+4\sqrt{3}}{8}\Delta N_3{}^{12}}$$
$$K_{c,3} = -\frac{T\Delta S}{\sum_{\alpha=1}^\infty\left(w(r_\alpha)\frac{\Delta N_\alpha^{12}}{2}\right)} = -\frac{T\Delta S}{\frac{3}{8}\frac{\Delta N_1^{12}}{2} + \frac{-1+2\sqrt{2}}{4}\frac{\Delta N_2^{12}}{2} + \frac{-3+4\sqrt{3}}{8}\frac{\Delta N_3^{12}}{2}} \quad (26)$$

Following the discussions in the Supporting Information, it can be inferred that $K_{c,1}$ and $K_{c,2}$ are all negative constants, while the sign of $K_{c,3}$ is determined by the ratio $N^{(2)}/N^{(3)}$. The above analyses provide important guidance for particle distribution control in mDPD systems. In other words, the occurrences of agglomeration, adsorption, and extraction should be determined by the combination of coefficients, which will be verified in the next section.

RESULTS

In this section, three different mDPD systems corresponding to the three types of distribution transition are discussed in Sec. III are constructed using the mdpd package in LAMMPS.[53] For each system, numerous simulations with different sets of $\{A_{ij}\}$ are conducted to examine the relationships between particle distribution and interparticle interactions predicted by the extended lattice model.

In all of the following simulations, the repulsive force amplitudes B are set to 40. The dissipative force amplitudes γ between particles are set to 1, with the exception that in the liquid−liquid interface case, γ for the second liquid phases is set to 50 to achieve a different viscosity.

Agglomeration. A binary mDPD system composed of 600 type-1 particles as dispersed phase and 7200 type-2 particles as continuous phase was constructed, with the simulation box of size 23.6 × 2.0 × 23.6 in reduced units. The total particle density is about 7, satisfying the approximation condition $r_c \doteq 2a$. Periodic boundary conditions are applied in three dimensions. In the initial state, all type-1 particles were uniformly dispersed in phase 2 as shown in Figure 1. Then, the system evolved to the equilibrium state.

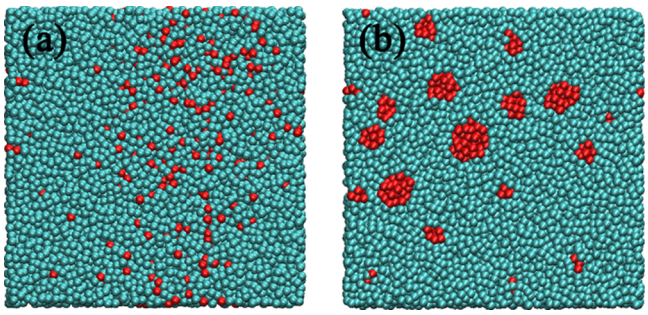

Figure 1. Particle distribution: (a) without agglomeration and (b) with agglomeration.

The degree of agglomeration is quantified in a similar way as in previous work,[54] dividing the simulation box into 10 × 1 × 10 blocks and calculating the relative standard deviation D of the number density of type-1 particles in each block

$$D = \sqrt{\frac{\sum_{i=1}^M (n_i/n_{ave} - 1)^2}{M-1}} \quad (27)$$

where M is the number of blocks, n_i is the number density of type-1 particles in block i, and n_{ave} is the average number density of type-1 particles. Then, simulations were conducted for 104 different models, where F_1 ranges from −30 to 30 with an interval of 5.

In Figure 2, it is indicated that the transition of the particle distribution from significant agglomeration to uniform dispersion happens as F_1 increases, which is consistent with the predictions of our model. The transition point K_c is in the interval [−10,0] and therefore negative, as estimated before. It is also observed that when the signs of the energetic and

https://doi.org/10.1021/acs.langmuir.3c01579
Langmuir 2023, 39, 17021−17030

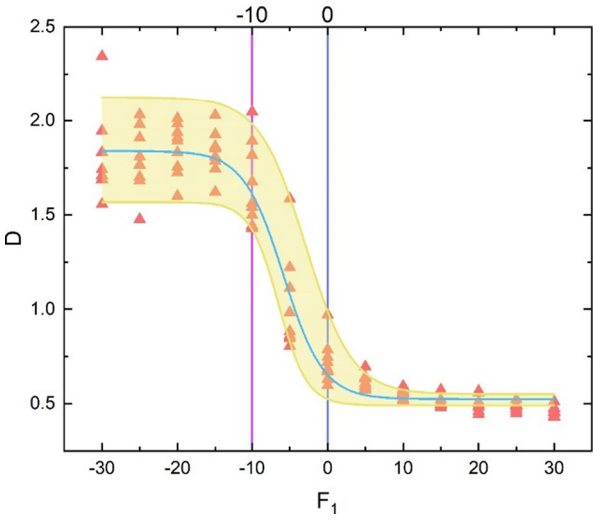

Figure 2. Degree of agglomeration as a function of the agglomeration factor $F_1 = -2A_{12} + A_{11} + A_{22}$. It is seen that when $F_1 < -10$, the relative standard deviation D of the number density of type-1 particles is scattered in the high-level range of 1.5 to 2.3, while when $F_1 > 0$, D decreases and converges to about 0.5. For the transition zone where $-10 < F_1 < 0$, D is distributed over a wide range from 0.6 to 2.0.

entropic contributions are opposite, namely, in the agglomeration state, the data points are more dispersed compared with the dispersed state. This is caused by the unknown correlations between the entropic contribution and the interparticle forces that influence the extent of agglomeration extent. While in the dispersed state, this entropic uncertainty is hidden by the energy counterpart because both terms tend to separate the particles uniformly in the continuous phases. As for the transition zone, when F_1 is close to K_c, accurate predictions of the distribution become impossible, for which there are several possible reasons. First, the free energy difference ΔF between different distributions in the transition zone could be comparable to the thermal energy, and the distribution becomes unstable due to the random particle motions. Besides, the inaccuracy could also be caused by the errors introduced from the lattice approximation in our model, and when the energy difference is not great enough to make the entropic and energetic errors negligible, the prediction loses its accuracy.

Adsorption on Solid Surfaces. In the extended lattice model, the adsorption of particles at the liquid−liquid interface and on the solid surface is considered to be the same process from the perspective of the Helmholtz free energy. However, in the real situation, the adsorption of particles at the liquid−liquid interface may also induce an extraction process, which would hinder the quantification of the adsorption extent. Therefore, in this section, only adsorption on the solid surface is considered to investigate the adsorption process independently, and adsorption at the liquid−liquid interface will be discussed together with extraction in the next section.

Here, a ternary mDPD system composed of 600 type-1 particles as the dispersed phase, 6400 type-2 particles as the liquid phase, and 7056 type-3 particles as the solid phase, with the simulation box of size 33.0 × 2.0 × 33.0 in reduced units, was constructed. Like the setup in Section VI.A, the approximation condition is fulfilled, and the periodic boundary conditions are applied. After equilibrium, all solid particles were simultaneously attached to their respective sites by spring forces at a given moment, and an additional linear repulsive force field was applied to all nonsolid particles entering the solid region, as in the literature.[55] Initially, all type-1 particles were uniformly dispersed in phase 2 as shown in Figure 3. Then, the system was allowed to evolve to the equilibrium state.

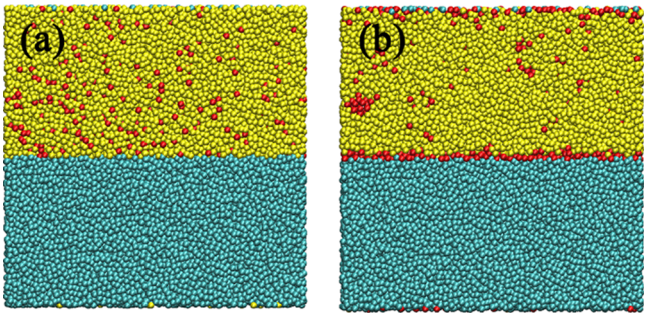

Figure 3. Particle distribution: (a) without adsorption on the solid surface and (b) with adsorption on the solid surface.

All of the type-1 particles with a distance less than r_c from the solid surface were regarded as being adsorbed. And the proportion of type-1 particles adsorbed on the solid surface X was used to quantify the degree of adsorption

$$X = \frac{N^S}{N^{(1)}} \tag{28}$$

where N^S is the number of type-1 particles adsorbed on the solid surface and $N^{(1)}$ is the total number of type-1 particles. The degrees of adsorption X in 112 models with F_2 ranging from −100 to 30, satisfying $F_1 > 0$ to avoid agglomeration in phase 2, were calculated.

From Figure 4, it is shown that as F_2 increases from −100 to 30, the particle distribution varies from the state with significant adsorption on the solid surface to the state without considerable adsorption, which agrees with our theory. As

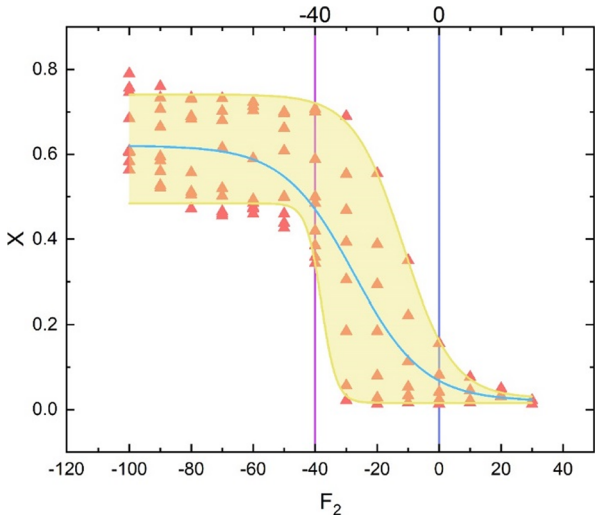

Figure 4. Degree of adsorption on the solid surface as a function of the adsorption factor $F_2 = A_{22} + A_{13} - A_{12} - A_{23}$. It is seen that when $F_2 < -40$, the degree of adsorption is diffusely distributed at a high level with an overall monotonically decreasing relationship to F_2, while when $F_2 > 0$, X is sharply reduced and approaches 0. In the transition zone between −40 and 0, X fluctuates in a wide range from 0.013 to 0.69.

https://doi.org/10.1021/acs.langmuir.3c01579
Langmuir 2023, 39, 17021−17030

predicted before, transition point K_c within the interval [−40, 0] is negative. Similar to the discussion made in the agglomeration case, here whether the energy and the entropy part are contributing to the free energy difference in the same direction or not induces the different degrees of dispersion of the data points between the two states. Besides, in our analysis, the dilute dispersion condition is employed, and it is assumed that no neighboring type-1 particles exist. However, Figure 3b shows that on the solid surfaces, type-1 particles aggregate and stack with each other, which does not satisfy our assumptions and may be another reason other than the entropic uncertainty for the inaccurate prediction within the transition zone. Generally, the above results demonstrate the validity of our theory in controlling the particle adsorption on solid surfaces, indicating that the additional force fields introduced to construct the solid model did not influence the thermodynamics of the adsorption processes. In the next section, the adsorption process at the liquid−liquid interfaces will be investigated.

Extraction and Adsorption at Liquid−Liquid Interfaces. In contrast to the solid−liquid interface in Section IV.B, here, a ternary mDPD system with a liquid−liquid interface was constructed, consisting of 600 type-1 particles as the dispersed phase, 6401 type-2 particles, and 6399 type-3 particles as two immiscible liquid phases. The simulation box was of size 33.8 × 2.0 × 33.8 in reduced units, and periodic boundary conditions are applied in three dimensions. In this section, the system was successively employed to investigate the extraction and adsorption processes.

To be specific, simulations on 130 different models with $F_1 > 0$ and F_3 ranging from −55 to 45 were first conducted to reveal the relation between the degree of extraction and F_3. Then, 85 models with F_2 ranging from −40 to 50 and $F_1 > 0$, $F_3 > 10$ to prevent agglomeration and extraction were constructed to investigate the adsorption at the liquid−liquid interface. As in Section IV.B, all type-1 particles in the initial state were uniformly dispersed in phase 2 as shown in Figure 5a, after which the system evolved to the equilibrium state.

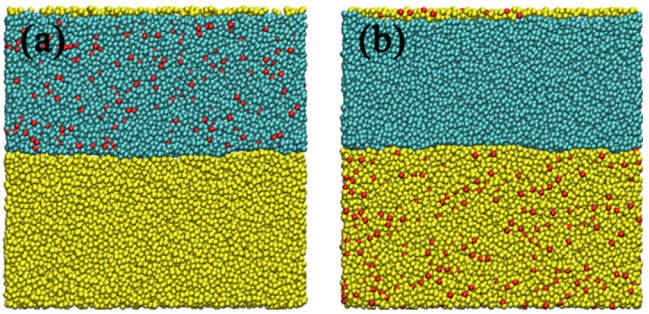

Figure 5. Particle distribution: (a) without extraction and (b) with extraction.

The degree of adsorption at the liquid−liquid interface is quantified in the same way as in the last section, by calculating the proportion of type-1 particles with a distance less than r_c from the liquid−liquid interface:

$$X = \frac{N^{L}}{N^{(1)}} \tag{29}$$

where N^{L} is the number of type-1 particles adsorbed at the liquid−liquid interface and N^{L} is the total number of type-1 particles. To quantify the degree of extraction, the proportion of type-1 particles immersed in phase 3 is calculated as:

$$I = \frac{N^{E}}{N^{(1)}} \tag{30}$$

where N^{E} is the number of type-1 particles extracted into phase 3.

The pattern presented in Figure 6 is similar to those in the previous section, which indicates the phase transfer of type-1 particles from phase 2 to phase 3 as F_3 decreases, as expected based on our model. Due to the close volume of phases 2 and 3, the sign of K_c is indeterminate, which is compatible with our theory (Figure 7).

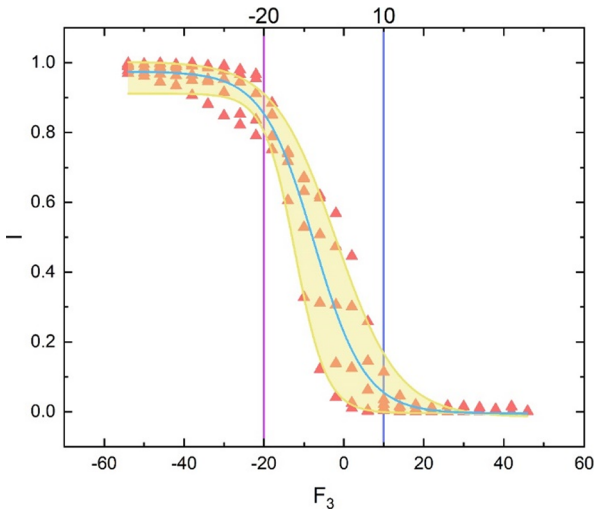

Figure 6. Degree of extraction as a function of the extraction factor $F_3 = A_{22} + 2A_{13} - A_{33} - 2A_{12}$. It is seen that I stays at a high level when $F_3 < -20$ and converges to 0 when $F_3 > 10$, while sharply decreasing with F_3 in the interval [−20,10].

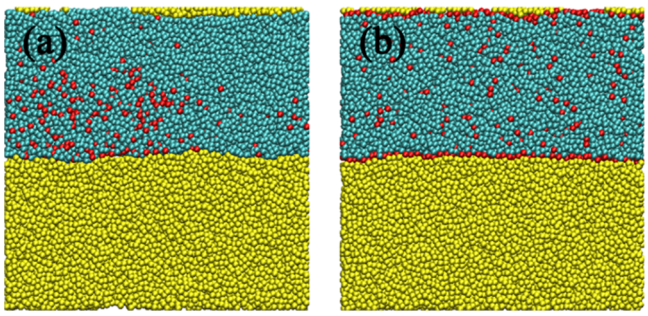

Figure 7. Particle distribution: (a) without adsorption at the liquid−liquid interface and (b) with adsorption at the liquid−liquid interface.

It is indicated in Figure 8 that $K_c < 0$, as predicted by our theory. Whereas here only models with $F_2 > -40$ were constructed and the distribution transition of the system was not fully presented. This limitation is caused by the fact that under the premise of no extraction, if we reduce F_2 to below −40, A_{23} will be increased to greater than 10 due to the coupling between F_2 and F_3, resulting in a significant decrease in the particle number density near the liquid−liquid interface and contradicting the assumption of an approximately uniform system density in our theoretical model. Hence, when

https://doi.org/10.1021/acs.langmuir.3c01579
Langmuir 2023, 39, 17021−17030

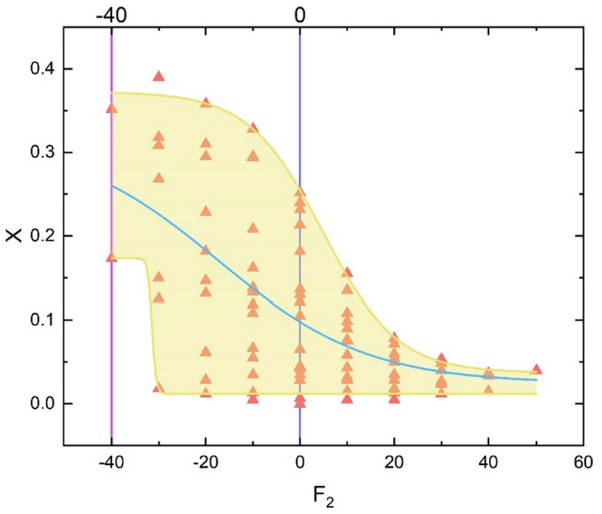

Figure 8. Degree of adsorption at the liquid−liquid interface as a function of the adsorption factor $F_2 = A_{22} + A_{13} - A_{12} - A_{23}$. When $F_2 > 0$, $X < 0.2$ and decreases to 0, in accordance with the pattern in the solid surface adsorption, indicating no significant adsorption at the liquid−liquid interface when $F_2 > 0$. When $-40 < F_2 < 0$, X is scattered in a wide range from 0 to 0.39, consistent with the distribution in the transition zone in Section IV.B.

investigating the adsorption at the liquid−liquid interface, the range of F_2 is limited, in contrast to solid surface adsorption, where no restriction of particle phase transfer is needed.

CONCLUSIONS

In this work, we extended Meyer's lattice model to describe dispersed multiphase systems and proposed an approximate formulation to estimate the Helmholtz free energy of the system. For agglomeration, adsorption, and extraction processes, the approximate free energy differences between the initial distribution and the final distribution are obtained. Based on the minimum free energy principle, the above free energy differences are used to derive three determinants $\Delta_i = F_i - K_{c,i}$ for the prediction of the preferable distribution of the system with given interparticle interaction potentials. The energy factors F_i describe the way interparticle potentials affect the energy change during distribution transitions, while the entropy factors $K_{c,i}$ are determined only by distribution changes, hence constant for given transitions. When $\Delta_i > 0$, which means the system with the final distribution has lower free energy, the distribution transition is predicted to take place and vice versa. To verify the above predictions for the three kinds of distribution transitions, a binary mDPD system, a ternary mDPD system with a liquid−solid interface, and a ternary mDPD system with a liquid−liquid interface were constructed to simulate the equilibrium distributions under different interaction settings. The simulation results showed notable monotonic dependence of the dispersed phase distributions on the three energy factors F_i and hence the determinants Δ_i as predicted by the criteria. Although the transition points $K_{c,i}$ could not be derived beforehand, their signs were predicted and verified by the simulation results. The good agreement between the theoretical predictions and the mDPD simulation results shows the great potential of our model for applications in the dispersed multiphase systems.

Compared to previous lattice models, which are restricted to binary isotropic mixtures, our model breaks the limit and can be applied to multicomponent anisotropic mixtures with interfaces considered. All the previous theories, including Meyer's model, Flory−Huggins theory, and the discussion made by Israelachvili, are based on the locality assumption, which ignores all the long-range interactions. In contrast, our model also considers cases in which long-range interactions are not negligible and proposes the corresponding analytical criteria based on a reasonable constraint on the form of the potential. However, like all of the previous lattice models, the quasi-uniform number density assumption is still needed, so the validity can only be guaranteed when applied to systems with small number density gradients like liquid mixtures. Besides, for the criteria of adsorption and extraction processes, the derivations are also based on the dilute dispersion assumption for simplicity. If condensed dispersion is considered, our lattice model and the general free energy difference formulation can still be employed but are expected to derive different and more complicated forms of criteria, which incorporate the interactions between particles of the dispersed phase.

In general, our model provides a novel and promising way to theoretically investigate dispersed multiphase systems with quasi-uniform number densities. The correlations between the distribution of the dispersed phase and the microscopic interparticle interactions are clarified, which have a wide range of applications in colloidal and interface science, like innovative nanoparticle synthesis, colloids characterization, and parameter control in particle-based simulations. More extensions can be made to our model, such as introducing voids into the lattice model to characterize systems with non-negligible number density variance, expressing the entropy factors with system parameters explicitly, and deriving criteria for more complicated distribution transition processes.

ASSOCIATED CONTENT

Supporting Information

The Supporting Information is available free of charge at https://pubs.acs.org/doi/10.1021/acs.langmuir.3c01579.

Detailed derivations of the particle distribution transition criteria for the agglomeration, adsorption, and extraction cases (PDF)

AUTHOR INFORMATION

Corresponding Author

Moran Wang − *Department of Engineering Mechanics, Tsinghua University, Beijing 100084, China;* orcid.org/0000-0002-0112-5150; Email: mrwang@tsinghua.edu.cn

Authors

Yiran Li − *Department of Engineering Mechanics, Tsinghua University, Beijing 100084, China*

Yunfan Huang − *Department of Engineering Mechanics, Tsinghua University, Beijing 100084, China*

Xukang Lu − *Department of Engineering Mechanics, Tsinghua University, Beijing 100084, China;* orcid.org/0000-0003-3315-6389

Complete contact information is available at: https://pubs.acs.org/10.1021/acs.langmuir.3c01579

Funding

This work was financially supported by the NSF grant of China (No. 12272207), the National Key R&D Program of China

(No. 2019YFA0708704), and the Tsinghua University Initiative Scientific Research Program.

Notes

The authors declare no competing financial interest.

REFERENCES

(1) Han, C. D. Multiphase Flow in Polymer Processing. In *Rheology: Volume 3: Applications*; Astarita, G.; Marrucci, G.; Nicolais, L. Eds.; Springer: US, 1980; pp 121−128.
(2) Derkach, S. R. Rheology of emulsions. *Adv. Colloid Interface Sci.* **2009**, *151* (1), 1−23.
(3) Kumar, S.; Yadav, I.; Aswal, V. K.; Kohlbrecher, J. Structure and interaction of nanoparticle−protein complexes. *Langmuir* **2018**, *34* (20), 5679−5695.
(4) Mashali, F.; Basham, C. M.; Xu, X.; Servidio, C.; Silva, P. H. J.; Stellacci, F.; Sarles, S. A. Simultaneous Electrophysiology and Imaging Reveal Changes in Lipid Membrane Thickness and Tension upon Uptake of Amphiphilic Gold Nanoparticles. *Langmuir* **2023**, *39*, 15031.
(5) Li, W.; Huberman-Shlaes, J.; Tian, B. Perspectives on Multiscale Colloid-Based Materials for Biomedical Applications. *Langmuir* **2023**, *39* (39), 13759−13769.
(6) Lei, W.; Lu, X.; Wang, M. Multiphase displacement manipulated by micro/nanoparticle suspensions in porous media via microfluidic experiments: From interface science to multiphase flow patterns. *Adv. Colloid Interface Sci.* **2023**, *311*, No. 102826.
(7) Pal, A.; Gope, A.; Iannacchione, G. Temperature and Concentration Dependence of Human Whole Blood and Protein Drying Droplets. *Biomolecules* **2021**, *11* (2), 231.
(8) Sun, X.; Zhang, Y.; Chen, G.; Gai, Z. Application of Nanoparticles in Enhanced Oil Recovery: A Critical Review of Recent Progress. *Energies* **2017**, *10*, 345.
(9) Lei, W.; Lu, X.; Wu, T.; Yang, H.; Wang, M. High-performance displacement by microgel-in-oil suspension in heterogeneous porous media: Microscale visualization and quantification. *J. Colloid Interface Sci.* **2022**, *627*, 848−861.
(10) Gheorghe, I.; Saviuc, C.; Ciubuca, B.; Lazar, V.; Chifiriuc, M. C. Nanodrug delivery systems for transdermal drug delivery. In *Nanomaterials for Drug Delivery and Therapy*; Elsevier: 2019; pp 225−244.
(11) Pei, X.; Song, W. CO2-Triggered Hierarchical-Pore UiO-66-Based Pickering Emulsions for Efficient and Recyclable Suzuki−Miyaura Cross-Coupling in Biphasic Systems. *Langmuir* **2023**, *39*, 15046.
(12) Testa, A.; Spanke, H. T.; Jambon-Puillet, E.; Yasir, M.; Feng, Y.; Küffner, A. M.; Arosio, P.; Dufresne, E. R.; Style, R. W.; Rebane, A. A. Surface Passivation Method for the Super-repellence of Aqueous Macromolecular Condensates. *Langmuir* **2023**, *39*, 14626.
(13) Chen, N.; Wang, Y.; Deng, Z. DNA-Condensed Plasmonic Supraballs Transparent to Molecules. *Langmuir* **2023**, *39* (39), 14053−14062.
(14) Xian, X.; Ye, Z.; Tang, L.; Wang, J.; Lai, N.; Xiao, B.; Wang, Z.; Li, S. Molecular Dynamics Simulation of the Effects of Complex Surfactants on Oil−Water Interaction and Aggregation Characteristics at the Interface. *Langmuir* **2023**, *39* (39), 14130−14138.
(15) Karishma, S.; Rajvanshi, K.; Kumar, H.; Basavaraj, M. G.; Mani, E. Oil-in-Water Emulsions Stabilized by Hydrophilic Homopolymers. *Langmuir* **2023**, *39* (38), 13430−13440.
(16) Vu, M. T.; Ngan Nguyen, T. T.; Hung, T. Q.; Pham-Truong, T.-N.; Osial, M.; Decorse, P.; Nguyen, T. T.; Piro, B.; Thu, V. T. Insights into Structural Behaviors of Thiolated and Aminated Reduced Graphene Oxide Supports to Understand Their Effect on MOR Efficiency. *Langmuir* **2023**, *39* (39), 13897−13907.
(17) Chakraborty, S.; Panigrahi, P. K. Stability of nanofluid: A review. *Appl. Therm. Eng.* **2020**, *174*, No. 115259.
(18) Jiang, D.; Chen, H.-B.; Qian, C.; Zhou, X.-L.; Liu, X.-W. Determining the aggregation kinetics of nanoparticles by single nanoparticle counting. *ACS ES&T Water* **2021**, *1* (3), 672−679.
(19) Wang, X.-J.; Zhu, D.-S Investigation of pH and SDBS on enhancement of thermal conductivity in nanofluids. *Chem. Phys. Lett.* **2009**, *470* (1−3), 107−111.
(20) Chakraborty, S.; Sarkar, I.; Ashok, A.; Sengupta, I.; Pal, S. K.; Chakraborty, S. Thermo-physical properties of Cu-Zn-Al LDH nanofluid and its application in spray cooling. *Appl. Therm. Eng.* **2018**, *141*, 339−351.
(21) He, Y. T.; Wan, J.; Tokunaga, T. Kinetic stability of hematite nanoparticles: the effect of particle sizes. *J. Nanopart. Res.* **2008**, *10*, 321−332.
(22) Luu, X. C.; Yu, J.; Striolo, A. Nanoparticles adsorbed at the water/oil interface: coverage and composition effects on structure and diffusion. *Langmuir* **2013**, *29* (24), 7221−7228.
(23) Dugyala, V. R.; Muthukuru, J. S.; Mani, E.; Basavaraj, M. G. Role of electrostatic interactions in the adsorption kinetics of nanoparticles at fluid-fluid interfaces. *Phys. Chem. Chem. Phys.* **2016**, *18* (7), 5499−5508.
(24) Bergfreund, J.; Sun, Q.; Fischer, P.; Bertsch, P. Adsorption of charged anisotropic nanoparticles at oil−water interfaces. *Nanoscale Adv.* **2019**, *1* (11), 4308−4312.
(25) Kysylychyn, D.; Piatnytsia, V.; Lozovski, V. Electrodynamic interaction between a nanoparticle and the surface of a solid. *Phys. Rev. E: Stat. Phys., Plasmas, Fluids* **2013**, *88* (5), No. 052403.
(26) Silva, R. M. E.; Poon, R.; Milne, J.; Syed, A.; Zhitomirsky, I. New developments in liquid-liquid extraction, surface modification and agglomerate-free processing of inorganic particles. *Adv. Colloid Interface Sci.* **2018**, *261*, 15−27.
(27) Yang, J.; Lee, J. Y.; Ying, J. Y. Phase transfer and its applications in nanotechnology. *Chem. Soc. Rev.* **2011**, *40* (3), 1672−1696.
(28) Milne, J.; Zhitomirsky, I. Application of octanohydroxamic acid for liquid-liquid extraction of manganese oxides and fabrication of supercapacitor electrodes. *J. Colloid Interface Sci.* **2018**, *515*, 50−57.
(29) Brader, J. M.; Dijkstra, M.; Evans, R. Inhomogeneous model colloid-polymer mixtures: adsorption at a hard wall. *Phys. Rev. E* **2001**, *63* (4 Pt 1), No. 041405.
(30) Bhattacharya, S.; Milchev, A.; Rostiashvili, V. G.; Grosberg, A. Y.; Vilgis, T. A. Adsorption kinetics of a single polymer on a solid plane. *Phys. Rev. E* **2008**, *77* (6Pt 1), No. 061603.
(31) Bakhshandeh, A.; dos Santos, A. P.; Levin, Y. Weak and strong coupling theories for polarizable colloids and nanoparticles. *Phys. Rev. Lett.* **2011**, *107* (10), No. 107801.
(32) Law, B.; Petit, J.-M.; Beysens, D. Adsorption-induced reversible colloidal aggregation. *Phys. Rev. E: Stat. Phys., Plasmas, Fluids* **1998**, *57* (5), 5782.
(33) Hill, T. L. Statistical Mechanics of Adsorption. IX. Adsorption Thermodynamics and Solution Thermodynamics. *J. Chem. Phys.* **1950**, *18* (3), 246−256.
(34) Wolf-Gladrow, D. A. *Lattice Gas Cellular Automata and Lattice Boltzmann Models: An Introduction*; Springer-Verlag: Berlin Heidelberg, 2000.
(35) Guo, Y.; Wang, M. Lattice Boltzmann modeling of phonon transport. *J. Comput. Phys.* **2016**, *315*, 1−15.
(36) Xie, C.; Lei, W.; Wang, M. Lattice Boltzmann model for three-phase viscoelastic fluid flow. *Phys. Rev. E: Stat. Phys., Plasmas, Fluids* **2018**, *97* (2), No. 023312.
(37) Flory, P. J. Thermodynamics of High Polymer Solutions. *J. Chem. Phys.* **1942**, *10* (1), 51−61.
(38) Kjellander, R. *Statistical Mechanics of Liquids and Solutions: Intermolecular Forces, Structure and Surface Interactions*; CRC Press: 2019.
(39) Fredrickson, G. H.; Liu, A. J.; Bates, F. S. Entropic corrections to the Flory-Huggins theory of polymer blends: Architectural and conformational effects. *Macromolecules* **1994**, *27* (9), 2503−2511.
(40) Israelachvili, J. N. *Intermolecular and Surface Forces*, 3rd ed.; Academic Press: 2011, DOI: 10.1016/C2009-0-21560-1.
(41) Zhao, J.; Chen, S.; Phan-Thien, N. Rheology of polymers in many-body dissipative particle dynamics simulations: Schmidt number effect. *Mol. Simul.* **2018**, *44* (10), 797−814.

(42) Kadoya, N.; Arai, N. Size dependence of static polymer droplet behavior from many-body dissipative particle dynamics simulation. *Phys. Rev. E: Stat. Phys., Plasmas, Fluids* **2017**, *95* (4), No. 043109.
(43) Ghoufi, A.; Malfreyt, P. Mesoscale modeling of the water liquid-vapor interface: a surface tension calculation. *Phys. Rev. E* **2011**, *83* (5 Pt 1), No. 051601.
(44) Arienti, M.; Pan, W.; Li, X.; Karniadakis, G. Many-body dissipative particle dynamics simulation of liquid/vapor and liquid/solid interactions. *J. Chem. Phys.* **2011**, *134* (20), 204114.
(45) Espanol, P.; Warren, P. B. Perspective: Dissipative particle dynamics. *J. Chem. Phys.* **2017**, *146* (15), 150901.
(46) Zhao, J.; Chen, S.; Zhang, K.; Liu, Y. A review of many-body dissipative particle dynamics (MDPD): Theoretical models and its applications. *Phys. Fluids* **2021**, *33* (11), 65538.
(47) Van Megen, W.; Snook, I.; Watts, R. Elastic properties of model colloids. *J. Colloid Interface Sci.* **1980**, *77* (1), 131−137.
(48) Masliyah, J. H.; Bhattacharjee, S. *Electrokinetic and colloid transport phenomena*; John Wiley & Sons: 2006.
(49) Chen, C.; Lu, K.; Li, X.; Dong, J.; Lu, J.; Zhuang, L. A many-body dissipative particle dynamics study of fluid−fluid spontaneous capillary displacement. *RSC Adv.* **2014**, *4*, 13.
(50) Warren, P. B. Vapor-liquid coexistence in many-body dissipative particle dynamics. *Phys. Rev. E* **2003**, *68* (6 Pt 2), No. 066702.
(51) Warren, P. B. No-go theorem in many-body dissipative particle dynamics. *Phys. Rev. E: Stat. Phys., Plasmas, Fluids* **2013**, *87* (4), No. 045303.
(52) Groot, R. D.; Warren, P. B. Dissipative particle dynamics: Bridging the gap between atomistic and mesoscopic simulation. *J. Chem. Phys.* **1997**, *107* (11), 4423−4435.
(53) Li, Z.; Hu, G.-H.; Wang, Z.-L.; Ma, Y.-B.; Zhou, Z.-W. Three dimensional flow structures in a moving droplet on substrate: A dissipative particle dynamics study. *Phys. Fluids* **2013**, *25*, No. 072103.
(54) Wang, Z.; Jin, X.; Wang, X.; Sun, L.; Wang, M. Pore-scale geometry effects on gas permeability in shale. *J. Nat. Gas Eng.* **2016**, *34*, 948−957.
(55) Henrich, B.; Cupelli, C.; Moseler, M.; Santer, M. An adhesive DPD wall model for dynamic wetting. *EPL.* **2007**, *80* (6), 60004.

https://doi.org/10.1021/acs.langmuir.3c01579
Langmuir 2023, 39, 17021−17030